processes

MDPI

Article

Low-Temperature Steam Reforming of Natural Gas after LPG-Enrichment with MFI Membranes

Dominik Seeburg †, Dongjing Liu †, Radostina Dragomirova, Hanan Atia, Marga-Martina Pohl, Hadis Amani, Gabriele Georgi, Stefanie Kreft and Sebastian Wohlrab *

Leibniz Institute for Catalysis at the University of Rostock, Albert-Einstein-Str. 29a, D-18059 Rostock, Germany; dominik.seeburg@catalysis.de (D.S.); liudongjing19@163.com (D.L.); radidragomirova@gmail.com (R.D.); hanan.atia@catalysis.de (H.A.); marga.pohl@freenet.de (M.-M.P.); hadis.amani@catalysis.de (H.A.); gabi.georgi@web.de (G.G.); stefanie.kreft@catalysis.de (S.K.)

* Correspondence: sebastian.wohlrab@catalysis.de; Tel.: +49-381-128-1328

† These authors contributed equally to this work.

Received: 15 November 2018; Accepted: 8 December 2018; Published: 12 December 2018

Abstract: Low-temperature hydrogen production from natural gas via steam reforming requires novel processing concepts as well as stable catalysts. A process using zeolite membranes of the type MFI (Mobile FIve) was used to enrich natural gas with liquefied petroleum gas (LPG) alkanes (in particular, propane and *n*-butane), in order to improve the hydrogen production from this mixture at a reduced temperature. For this purpose, a catalyst precursor based on Rh single-sites (1 mol% Rh) on alumina was transformed in situ to a $Rh1/Al_2O_3$ catalyst possessing better performance capabilities compared with commercial catalysts. A wet raw natural gas (57.6 vol% CH_4) was fully reformed at 650 °C, with 1 bar absolute pressure over the $Rh1/Al_2O_3$ at a steam to carbon ratio S/C = 4, yielding 74.7% H_2. However, at 350 °C only 21 vol% H_2 was obtained under these conditions. The second mixture, enriched with LPG, was obtained from the raw gas after the membrane process and contained only 25.2 vol% CH_4. From this second mixture, 47 vol% H_2 was generated at 350 °C after steam reforming over the $Rh1/Al_2O_3$ catalyst at S/C = 4. At S/C = 1 conversion was suppressed for both gas mixtures. Single alkane reforming of C_2–C_4 showed different sensitivity for side reactions, e.g., methanation between 350 and 650 °C. These results contribute to ongoing research in the field of low-temperature hydrogen release from natural gas alkanes for fuel cell applications as well as for pre-reforming processes.

Keywords: steam reforming; pre-reforming; alkanes; hydrogen; membrane separation; single-sites

1. Introduction

Exploitation of the world's reserves of natural gas has increased tremendously, while the spectrum of utilization has broadened continuously. Methane, the main component in natural gas, is typically combusted for energy generation, since it is difficult to activate this smallest alkane and form more valuable products [1]. In terms of direct methane activation, several directions can be pursued which are currently only of academic interest [2–6]. Hence, for chemical processing, methane is mainly converted into H_2/CO mixtures (syngas) which provide key components for the production of chemical products [7–10], e.g., for the synthesis of ammonia, methanol, and liquid hydrocarbons [11]. The steam reforming process of methane is typically performed at high temperatures between 750 and 900 °C. At a pressure of p = 24 bar and a steam to carbon ratio of S/C = 3, nearly 75 vol% H_2 is produced (excluding water) [12].

Wet natural gas, rich in C_2–C_5 alkanes, or C_2–C_5 alkane fractions from natural gas conditioning, are valuable sources for syngas production. Depending on the alkane composition and the processing

technology (i.e., steam reforming, partial oxidation, autothermal reforming, dry reforming), syngas with different H_2/CO ratios can be obtained by using suitable catalysts [13]. Generally, the highest possible amount of H_2 can be achieved by using steam as a reactant for alkanes, due to the inherent hydrogen content of the water. Industrially, pre-reforming of the higher alkanes in wet natural gas can help to reduce the size of a downstream tubular reformer [9]. Moreover, liquid fuels such as butane, alcohols, or diesel are increasingly being considered as easily storable sources of hydrogen which can be applied in fuel cell systems [14–18]. Among those, reforming of bioethanol could contribute to sustainable hydrogen production. However, a high temperature of about 700 °C is required to obtain hydrogen yields above 70% [19].

Steam reforming of alkanes requires a significant energy input [20,21]. For methane conversion, the required ΔH° is +206 kJ/mol [22], hence, the reaction has to be performed at high temperatures (often higher than 900 °C) to ensure full conversion [23]. In order to decrease the required reaction temperature, low pressure and a relatively high S/C ratio are necessary [14]. Several attempts have been made in order to lower the required energy input for alkane steam reforming [22]. Interestingly, the reforming of higher alkanes can be performed at a lower temperature compared to methane. For instance, complete conversion of *n*-butane can be achieved at 405 °C over Pt-Ni/δ-Al_2O_3 [15]. Schädel et al. [20] systematically tested an industrial Rh catalyst as a washcoat on cordierite honeycomb monoliths for the steam reforming of methane, ethane, propane, butane, and natural gas. The authors showed that methane requires a much higher temperature for conversion compared to the other alkanes. Consequently, steam reforming of a natural gas with a high liquefied petroleum gas (LPG) fraction would offer lower reaction temperatures.

The enrichment of natural gas with LPG alkanes via MFI (Mobile FIve)-membranes has been reported in the past. Selective gas transport across zeolite membranes can be achieved by either selective adsorption or size exclusion [24]. Due to their selective adsorption properties, MFI zeolite membranes are extensively studied for separation of different alkanes [25–29]. From a mechanistic point of view, the higher molecular weight alkanes adsorb preferentially at the membrane surface and thus block the pores for further passage of lighter components. However, a fundamental understanding of transport across the membrane and the accurate analysis of optimal operating parameters are essential for achieving high membrane performances. The separation of natural gas alkanes based on the adsorption behavior of the different alkanes was first demonstrated by Arruebo et al. [30] and detailed parameter studies were performed by our group [31–34].

Unfortunately, stable catalysts working at lower temperatures in the steam reforming of LPG enriched natural gas are rather scarce. Carbon deposition, the most serious problem affecting the stability of catalysts at low reaction temperatures (400–550 °C), was investigated by Angeli et al. [35] who found significant carbon residues on Ni catalysts, while in the presence of Rh, coke was oxidized. Our initial idea was to reduce the size of the active sites in order reduce coking ability. In terms of methane activation, Bao and co-workers developed an oxygen free route towards C_2 and aromatic products over Fe single-sites [36]. Moreover, direct transformation of methane to methanol can be performed over Pd single-sites at a low temperature [37], or over single-site copper species in zeolites [38–41]. Molecularly attached VO_x single-sites on silica have been used as catalysts for the selective oxidation of methane towards formaldehyde [42–44]. However, in terms of steam reforming of methane, Bokhoven and co-workers recently found that the catalytic reaction over single Rh sites on stabilizing supports requires additional nanoparticles to oxidize formed carbon species [45]. In the absence of nanoparticles, reaction rates are lowered due to the formation of carbon species which are strongly bound to the surface.

In this work, we started with single Rh site rhodium catalyst precursors in the steam reforming of alkanes and LPG rich natural gas. The single-sites were transformed during the reaction and the in situ formed catalysts containing Rh nanoparticles surprisingly delivered a much better performance compared to commercial catalysts at low temperature. Therefore, a membrane-based pre-enrichment

of LPG can be introduced as a feasible concept to obtain an alkane mixture from which a high amount of hydrogen can be produced at temperatures as low as 350 °C.

2. Materials and Methods

2.1. Catalyst Preparation

Rh1/Al_2O_3 with 1.0 mol% Rh was prepared by impregnation of Al_2O_3. First, 15 g Disperal P2 (Sasol, Brunsbüttel, Germany) were calcined at 800 °C (heating rate 5 °C/min) for 90 min in air. Afterwards, the as-obtained Al_2O_3 was impregnated with a freshly prepared $Rh(NO_3)_3$ solution. Accordingly, 1.9 g $RhCl_3 \cdot 4.5H_2O$ (Alfa Aesar, Karlsruhe, Germany) were dissolved in 100 mL of water. The solution was heated and 20 mL of aqueous 20 M KOH (Fisher Chemical, Loughborough, UK) were added dropwise under reflux. The precipitated $Rh(OH)_3$ was centrifuged and washed four times with hot water. The resulting $Rh(OH)_3$ precipitate was then dissolved in 5 mL of concentrated HNO_3 (Fisher Chemical, Loughborough, UK) and subsequently diluted in 20 mL of deionized water to obtain a $Rh(NO_3)_3$ concentration of about 0.35 mol/L. As a last step, 2.85 mL of this solution was further diluted in 47.2 mL of deionized water and used for the wet impregnation of 10 g of Al_2O_3. This slurry was stirred for 1 h, water was subsequently removed using a rotary evaporator, and the resulting catalyst was dried over night at 110 °C. Finally, calcination of the material was performed at 700 °C in air for 60 min (heating rate 5 °C/min). The catalysts were abbreviated as follows: Rh1/Al_2O_3 for 1.0 mol% Rh on alumina. Several other loadings of Rh on alumina were abbreviated as Rh_X/Al_2O_3 with (x = 0.01, 0,1, and 0.5 in mol% Rh, determined via inductively coupled plasma - optical emission spectroscopy ICP-OES). For comparison, two commercial catalysts consisting of 0.5 % Rh (206172) on alumina and 5% Rh (C-301099-5) on alumina were purchased from Sigma-Aldrich (Steinheim, Germany) and Alfa Aesar (Karlsruhe, Germany), respectively, and tested under comparable conditions.

2.2. Catalyst Characterization

The BET (Brunauer–Emmett–Teller) specific surface area of the porous silica and the catalysts were measured by N_2 adsorption using a NOVA 4200e instrument from Quantachrome (Odelzhausen, Germany). As a pre-treatment, samples were outgassed and dried for 2 h at 200 °C at reduced pressure.

Powder X-ray diffraction (XRD) patterns of the calcined samples were measured in the angle range 5–80° 2Theta scale on a Theta/Theta diffractometer X'Pert Pro (Panalytical, Almelo, Netherlands) using a Ni-filtered Cu–K_α radiation (λ = 1.5418 Å, 40 kV, 40 mA). The data were recorded with the X'Celerator (RTMS) detector.

Transmission electron microscopy (TEM) measurements at 200 kV were performed on a JEM-ARM200F (JEOL) with aberration-correction by a CESCOR (CEOS) for the scanning transmission (STEM) applications (JEOL, Corrector: CEOS, Tokyo, Japan).

A Varian 715-ES ICP-OES (Inductively Coupled Plasma-Optical Emission Spectrometer) (Varian Palo Alto, CA, USA) was used for the determination of the elemental composition of the catalysts. Before analysis, the catalysts were completely dissolved in a solution containing 8 mL of aqua regia and 2 mL of hydrofluoric acid.

The H_2-TPR (temperature programmed reduction with H_2) experiments were done as described in the following. 160 mg of the respective sample was loaded in a u-shaped quartz reactor and heated from RT (room temperature) to 500 °C at 20 K/min in air, then cooled to RT and flushed with Ar flow (50 mL/min) for 30 min. H_2-TPR of Rh1/Al_2O_3 samples were carried out from 0 to 800 °C in a flow of 5% H_2/Ar (20 mL/min) with a heating rate of 5 K/min. The temperature was held at 800 °C for 1 h. The hydrogen consumption peaks were recorded simultaneously via a thermal conductivity detector (TCD, ChemiSorb 2920-Instrument, Mircomeritics, Norcross, GA, USA).

2.3. Membrane Separation

Pressure-stable and defect-free MFI membranes at the inner side of porous alumina tubes (l = 125 mm, d_{outer} = 10 mm, d_{inner} = 8 mm) were prepared via a secondary growth procedure previously reported by our group in Reference [31]. The tubes were sealed with glass at both ends and embedded in stainless steel permeation cells with Viton O-rings. LPG enrichment from natural gas using the MFI membranes was performed at $p_{permeate}$ = 0.17 bar, p_{feed} = 7 bar, and T = 75 °C. Compositions of permeate and retentate were analyzed continuously using an online coupled capillary GC HP 6890 from Hewlett Packard (Santa Clara, CA, USA).

2.4. Catalytic Steam Reforming Tests

Steam reforming of alkanes, alkane mixtures, and simulated natural gas (before and after membrane enrichment) were performed in a vertical fixed bed plug flow quartz reactor (l = 260 mm, d_{inner} of 8 mm) at 1 bar (detailed composition of the reaction mixtures are given in Table S1 and S2). If not otherwise stated, 150 mg of catalyst was fixed with quartz wool at the centre of the reactor tube and heated in a furnace at temperatures ranging from 200 to 850 °C. If not otherwise stated, the holding time spent for each temperature set point was about 35 min. Temperature was controlled by two thermocouples (ThermoExpert, Stapelfeld, Germany) at the outer reactor wall and in the middle of the catalyst bed. The gas flow was controlled by mass flow controllers (MKS, Andover, MA, USA). The total gas flow under ambient conditions of 100 cm^3 min^{-1} consisted of 25 cm^3 min^{-1} of reactant gas (steam and alkanes) diluted in 75 cm^3 min^{-1} of nitrogen to reach near isothermal conditions. If not otherwise stated, GHSV (gas hourly space velocity) was about 8000 h^{-1}. The required water was dosed to a vaporizer using a syringe pump at the front inlet of the reactor. All the transfer lines were heated at 130 °C. At the reactor outlet, water was condensed from the product gas stream in a cold trap at 0 °C. Gas phase products were analyzed by an online-GC 7890A (Agilent, Santa Clara, CA, USA). H_2, N_2, and CO were separated with a molsieve column 5Å from Agilent (CP-1306) (Santa Clara, CA, USA) and detected with a TCD. The alkanes and CO_2 were separated with a GS-Q column from Agilent (113-3432) (Santa Clara, CA, USA) and detected with a flame ionization detector (FID, Agilent, Santa Clara, CA, USA) with a methanation unit. For quantification of H_2, N_2, CO, CO_2, and C_1–C_5 alkanes, an external calibration was done with several test gas mixtures (supplied from Linde Group, Pullach, Germany) and their dilutions in N_2, as well as by measuring the pure gases. For discussion, H_2O and N_2 were excluded in the given volumetric gas compositions.

3. Results

3.1. $Rh1/Al_2O_3$ Catalyst

Rh single-atoms were deposited on a high surface alumina support of 181 m^2/g. The BET surface areas and pore volumes of the obtained $Rh1/Al_2O_3$ catalyst, given in Table 1, are only less affected after calcination, indicating the integrity of the support material after thermal treatment. The molar fraction of Rh in $Rh1/Al_2O_3$ was 1.0 mol%, which is in the range of the targeted value. X-ray diffraction patterns of the catalyst (Figure S1) shows only typical reflections of different alumina phases, namely, γ-, δ-, and θ-Al_2O_3 (JCPDS 29-0063 [46], PDF 46-1215 [47], and ICSD#082504 [48]).

Table 1. BET (Brunauer–Emmett–Teller) specific surface area (S_{BET}), total pore volume (V_t), and average pore diameter (D), as well as ICP-OES (inductively coupled plasma - optical emission spectroscopy) data of support and catalysts.

Samples	BET			ICP
	S_{BET} (m^2/g)	V_t (mL/g)	D (nm)	Rh (mol%)
Al_2O_3	181	0.413	9.1	-
$Rh1/Al_2O_3$	169	0.406	9.6	1.0

High-angle annular dark-field—scanning transmission electron microscopy (HAADF-STEM) images of fresh and spent catalysts are shown in Figure 1a,b. The spent catalysts were isolated after the light-off test with permeate gas at S/C = 4, running the reaction from 200 to 850 °C. In fresh $Rh1/Al_2O_3$, many visible Rh atoms well-dispersed over the γ-Al_2O_3 support and islands of single-sites can be detected (bright spots in yellow circles). Rh nanoparticles in the size of 1–3 nm are visible in the spent $Rh1/Al_2O_3$ catalyst, indicating particle formation from Rh single-sites during the steam reforming process.

H_2-TPR was performed with fresh and spent catalysts. The spent catalysts were isolated again after the light-off tests with permeate gas at 850 °C (S/C = 4). As can be concluded from Figure 1c, the absence of typical reduction peaks for particulate RhO_x species in the range from 80 to 250 °C [49,50] indicate the nature of the sites in fresh $Rh1/Al_2O_3$. Most Rh species in the fresh catalysts are present as single atoms, because the adsorption and dissociation of H_2 to H atoms cannot occur over single atoms [51]. H_2-TPR over spent $Rh1/Al_2O_3$ catalysts is in accordance with the TEM results. It is obvious that the single-sites in the fresh catalysts were transformed to nanoparticle species during an initial activation phase. The formed Rh particles in spent $Rh1/Al_2O_3$ show an extraordinary reducibility below 50 °C and were the active catalyst species.

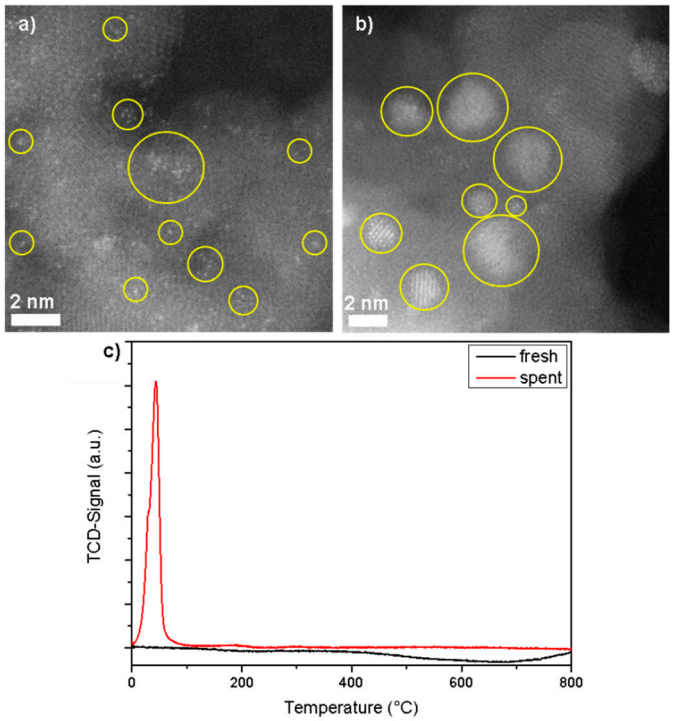

Figure 1. Catalyst characterization. High-angle annular dark-field—scanning electron microscopy (HAADF-STEM) images: (**a**) fresh $Rh1/Al_2O_3$, (**b**) spent $Rh1/Al_2O_3$, and (**c**) H_2-TPR (temperature programmed reduction with H_2) profiles of fresh and spent $Rh1/Al_2O_3$. Spent catalysts were isolated after hydrogen production from liquefied petroleum gas (LPG)-enriched permeate natural gas with a steam to carbon ratio (S/C) = 4, heating from 200 to 850 °C.

3.2. Steam Reforming of pure $C_{1–4}$ Alkanes and Mixtures of $C_{2–4}$ with Methane over $Rh1/Al_2O_3$

Steam reforming of the single alkanes methane, ethane, propane, *n*-butane, and *i*-butane were performed over $Rh1/Al_2O_3$ using S/C ratio and temperature as a measure for catalyst activity (Figure 2) and selectivity (Figure 3). At a GHSVs of 8000 h^{-1}, 1 mol% Rh appeared as sufficient loading to reach nearly equilibrium methane conversion [22] (Figure S2). At lower Rh loading, GHSVs have to be reduced to fulfil this task (e.g., Figures S3 and S4 for $Rh_{0.5}/Al_2O_3$). In the temperature range 250–400 °C, increasing S/C ratios lead to higher H_2 fractions in the product gas and higher alkanes

yield higher H_2 fractions than methane reforming. Above 500 °C, increasing methane conversion leads to higher H_2 fractions due to higher hydrogen/carbon-ratios in such mixtures. Between 550 and 850 °C, the respective H_2 fractions remain nearly constant between 70 vol% and 80 vol% at S/C = 4.

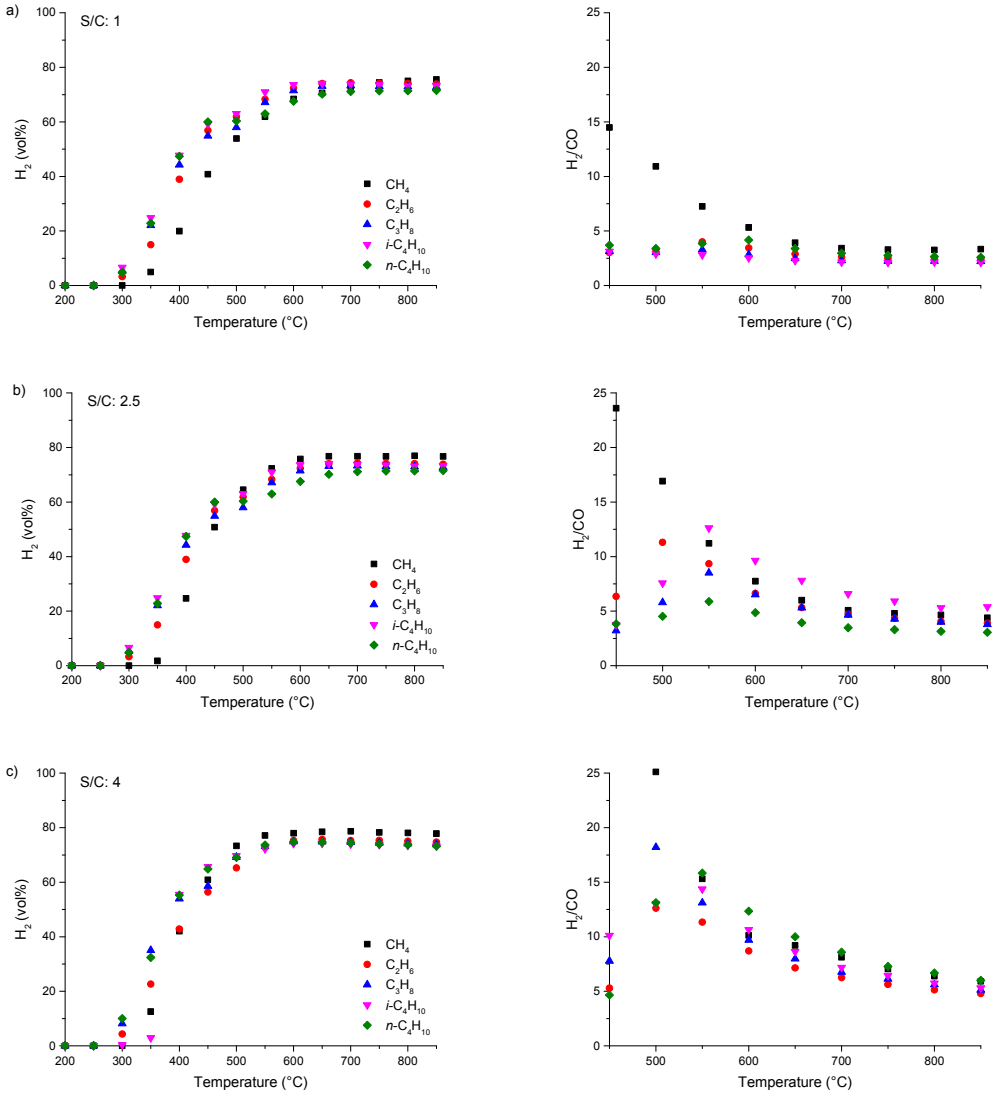

Figure 2. H_2 volumetric gas content (water and inert gas excluded) and H_2/CO ratio in the steam reforming of single alkanes over $Rh1/Al_2O_3$ at GHSV (gas hourly space velocity) of 8000 h^{-1} and different values of temperature and S/C ratios of (**a**) 1, (**b**) 2.5, and (**c**) 4.

The obtained H_2/CO ratios (Figure 2) also depend strongly on the S/C ratio and temperature. The H_2/CO ratios from methane steam reforming decrease with increasing temperature and decreasing S/C ratios. A more difficile behavior was found for $C_{2–4}$ alkanes. For many of those, a maximum H_2/CO ratio was observed around 500–600 °C, whereby the values increase with increasing S/C ratios. This region relates to the aforementioned side reactions, namely the water–gas shift reaction as well as the formation of CH_4. Concerning the latter, the amount of formed methane from C_2–C_4 alkanes dependent on the temperature and S/C ratio is depicted in Figure 3. At S/C = 1, the potential to form methane goes along the following order of the alkanes: Ethane~propane > *i*-butane > *n*-butane, reaching values up to ~30 vol% methane, and is most pronounced between temperatures of 500 and 600 °C. For higher S/C ratios another trend is observed according to ethane~propane > i-butane~*n*-butane. The CH_4 formation can be suppressed by increasing the amount of steam. Different mechanisms

can be responsible for CH_4 formation. Schädel et al. [20] observed CH_4 formation during the steam reforming of different higher alkanes over Rh catalysts and concluded that CH_4 is formed faster from higher hydrocarbons than decomposed, due to its lower reactivity at low temperatures. In addition, CO (and CO_2) hydrogenation by formed H_2 or the so-called methanation, also contributes to CH_4 production. Although the hydrogenolysis reaction is discussed as mostly being responsible for CH_4 production [52], methanation can also contribute to a significant loss of CO and consequently very high H_2/CO ratios. This feature could be suppressed to a certain extend by LPG enrichment as discussed later. As a direct consequence of CH_4 formation from the higher alkanes, two temperature regions can be defined for our approach: (i) before CH_4 formation in a low-temperature region, e.g., up to 350 °C and (ii) a high-temperature region when the formed CH_4 is completely reformed starting at 650 °C.

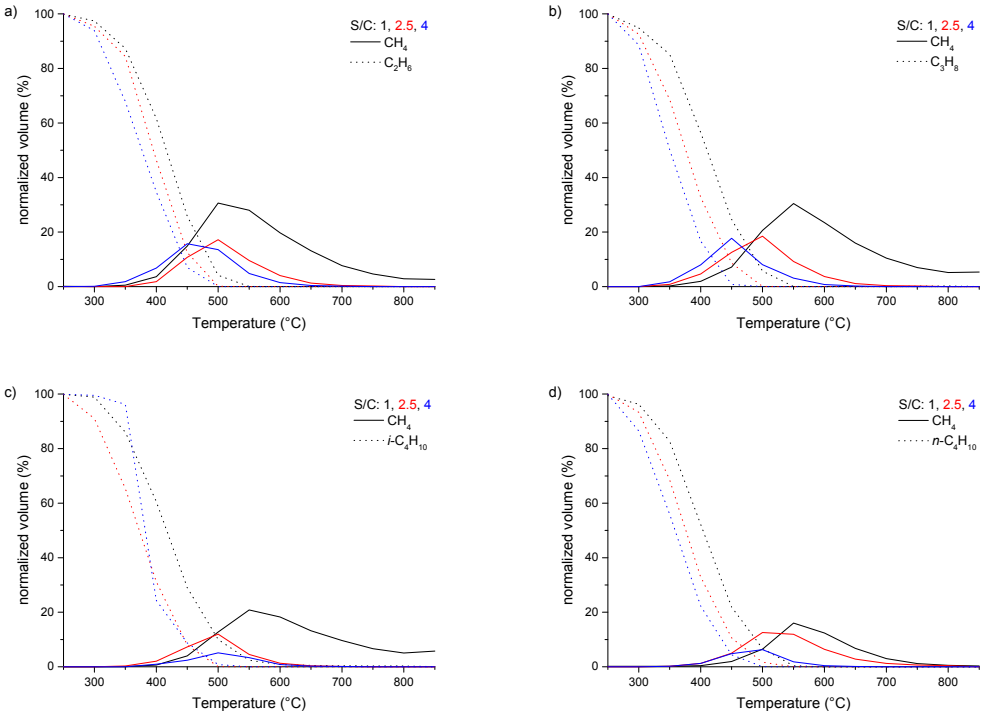

Figure 3. Formation of methane during steam reforming of (**a**) ethane, (**b**) propane, (**c**) *i*-butane and (**d**) *n*-butane over Rh1/Al_2O_3 at various S/C ratios and temperatures at a constant GHSV of ~8000 h^{-1}.

Finally, steam reforming tests of binary alkane mixtures with methane, namely, ethane/methane, propane/methane, and *n*-butane/methane, were performed at 350 °C over Rh1/Al_2O_3 to demonstrate the impact of higher alkanes on the achievable H_2 fractions and H_2/CO ratios (Figures S4 and S5). At this temperature, no methane is being formed from the higher alkanes. In general, an increasing content of higher alkanes causes a rise in the respective H_2 fractions. In the case of ethane/methane mixtures, for instance, the H_2 fractions increase from 5.0 vol% to 8.7 vol% (S/C = 1) when the volume fraction of ethane is increased from 0 to 100%. At the S/C ratio of 2.5, the H_2 fraction can be increased from 8.4 vol% to 15.0 vol% and even from 12.6 vol% to 22.6 vol% when the S/C ratio is further increased to 4. However, in the same way, the H_2/CO ratios decrease from 3.3 to 2.4 (S/C = 1), 4.6 to 3.9 (S/C = 2.5), and 5.9 to 4.8 (S/C = 4). Lower H_2/CO ratios at low methane content are attributed to (i) the reduced hydrogen/carbon-ratios and (ii) high CO selectivity of Rh1/Al_2O_3. The latter has already been demonstrated for the *n*-butane steam reforming in low-temperature range over Rh catalysts [53].

3.3. Enrichment of LPG from Natural Gas Using MFI-Membranes

Compared to presently used methods of recovering heavier hydrocarbons from methane [54], a membrane process offers a low energy consuming alternative. In this work, a wet natural gas (raw gas) was enriched with propane and *n*-butane (permeate gas; enriched with LPG) using a pressure stable MFI zeolite membrane. The compositions of the raw gas (sour gas and inert gas depleted, water-free) and permeate gas are depicted in Scheme 1. The subsequent steam reforming was performed in a separate reactor, since both operations require different working temperatures [55] (Scheme 1).

In the membrane process, pores are blocked for methane due to the preferred adsorption of LPG alkanes in the MFI structure and permeation is induced by a present gradient of the chemical potential, preferably by differences between permeate and feed pressure. At $p_{permeate}$ = 0.17 bar and p_{feed} = 7 bar (T = 75 °C), propane and *n*-butane enrichment of 37.6 vol% and 22.6 vol% in permeate from initial 18.9 vol% and 4.9 vol%, respectively, was obtained. *i*-butane hardly passes the MFI membrane as it is trapped in the zick-zack-channels of the zeolite [56], which is reflected in a lower amount of this component in the permeate.

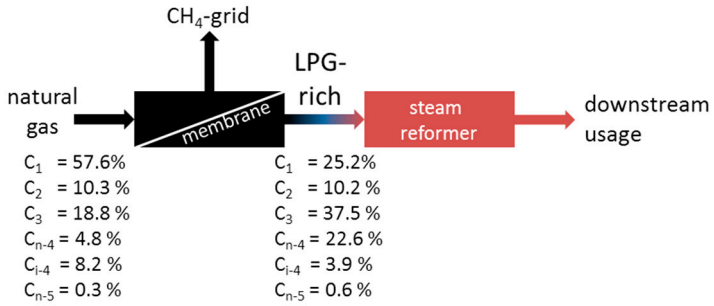

Scheme 1. Two-step process for the generation of hydrogen from wet natural gas, including membrane-based LPG-enrichment and further steam reforming.

3.4. Steam Reforming of Real Natural Gas Mixtures over $Rh1/Al_2O_3$

The product gas distributions obtained after steam reforming of the two gas mixtures over $Rh1/Al_2O_3$ (S/C = 1 and 4, GHSV~8000 h^{-1}) are displayed dependent on temperature in Figure 4. At S/C = 1 the reforming of raw gas starts at 350 °C and full conversion of higher alkanes is achieved at temperatures above 450 °C. With elevation of the reaction temperature, further methane conversion and rising H_2 and CO_x concentrations are observed. Nearly full methane conversion is reached at a temperature of 850 °C. At S/C = 4, complete conversion of higher alkanes and methane occurs at lower temperatures compared to the case of S/C = 1, and the respective H_2 concentration exhibits 76 vol% at 550 °C and levels off at higher reaction temperatures.

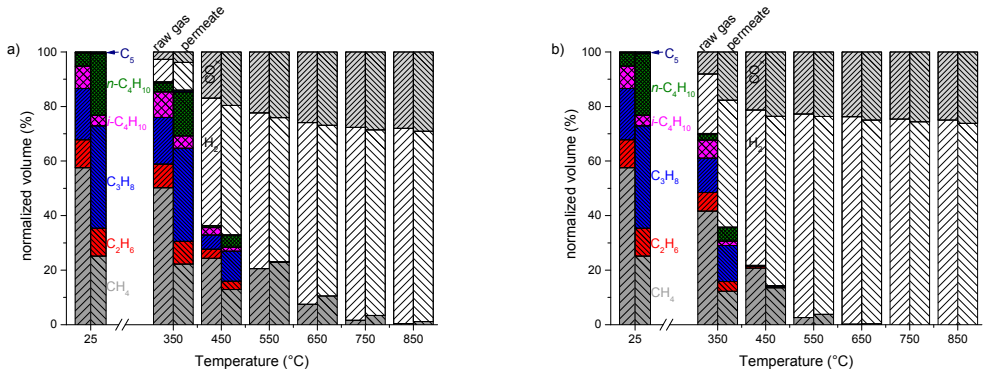

Figure 4. Volumetric gas contents of raw natural gas and LPG-enriched permeate natural gas from membrane pre-separation and after steam reforming over $Rh1/Al_2O_3$ at (**a**) S/C ratio of 1 and (**b**) S/C ratio of 4.

The product gas distribution resulting from the steam reforming of the permeate gas differs positively from that of the raw gas at low temperature, due to the higher LPG fraction in the mixture. Compared to the raw gas reforming, twice the concentration of H_2 is achieved from permeate gas reforming at 350 °C and S/C = 4 (H_2 concentration of 46.5%). Under such reaction conditions, $Rh1/Al_2O_3$ performs even better than a commercial catalyst consisting of 5% Rh on alumina (Figure S6). At 550 °C higher alkanes are nearly completely converted.

The related H_2 fractions, H_2/CO ratios, and CO/CO_2 volumetric contents are additionally depicted in Figures S7–S9. For both raw gas as well as permeate gas, the achievable H_2/CO ratios show a maximum between 500 and 550 °C, and gradually decrease with the elevation of temperatures above 550 °C. H_2/CO ratios obtained from permeate gas reforming are slightly lower than those from raw gas transformation. At S/C = 4 the CO/CO_x-ratio (Figure S9) presents the most significant minimum at 500 °C, leading to H_2/CO ratios far above 10, which point to the side reactions which were described earlier.

Time-on-stream performance of $Rh1/Al_2O_3$ in the steam reforming of LPG-enriched permeate natural gas at 350 °C and 850 °C (S/C ratio = 4) is displayed in Figure 5. The activity of $Rh1/Al_2O_3$ increases during the first hour on stream and is nearly stable in the subsequent reaction time.

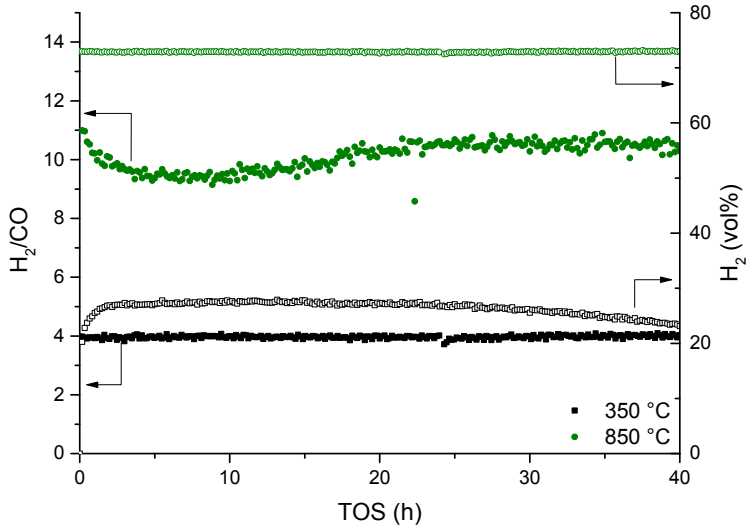

Figure 5. Steam reforming of permeate natural gas over $Rh1/Al_2O_3$ at S/C ratio of 4 and temperatures of 350 and 850 °C.

This behaviour is not in accordance with general considerations regarding catalyst deactivation [57]. Commonly, particle deactivation involves (i) a loss in surface area in the beginning of the reaction, (ii) slowed sintering on stream, and (iii) reaching a stable performance at a certain time. In the present case, the active phase, e.g., formed nanoparticles from Rh single-sites, is being created during the initial stage and seems to possess particularly suitable features for the reaction at low temperatures. At 850 °C, $Rh1/Al_2O_3$ shows no deactivation over 40 h on stream, the hydrogen yield remains at ~73 vol%, and the H_2/CO ratio was constant at 4.

4. Conclusions

A highly active Rh catalyst was formed in situ on Al_2O_3 during the reaction of C_1–C_5 alkanes with steam. The active phase in $Rh1/Al_2O_3$ were Rh nanoparticles in the range 1–3 nm formed from single Rh-atoms. The product spectrum of steam reformed alkanes over $Rh1/Al_2O_3$ strongly depends on S/C ratios and temperatures. With this catalyst, an alkane mixture of an LPG-rich natural gas containing 57.8 vol% CH_4 can be fully reformed at 650 °C at S/C = 4. Below 650 °C, the higher alkanes showed a positive impact on the hydrogen production from binary mixtures at low temperatures

but contributed to methanation. Furthermore, maximum H_2/CO ratios (>10) were detected between 350 and 650 °C. Consequently, pre-reforming of LPG-rich natural gas should be performed under very mild conditions, no higher than 350 °C. Therefore, the application of a membrane-based pre-separation represents a feasible concept to obtain (i) easily activatable LPG-enriched natural gas for hydrogen production and (ii) a purified methane fraction for possible injection into the gas grid. Exemplarily, the enrichment of the C_2–C_5 alkane fraction (remaining 25.2 vol% CH_4) in the permeate gas leads to further enhancement of the steam reforming reaction. At low reaction temperatures as low as 350 °C (S/C = 4), the volumetric hydrogen content in the product was increased from 21.8% to 46.5 vol% at a reasonable H_2/CO ratio of 4.7.

Supplementary Materials: The following are available online at http://www.mdpi.com/2227-9717/6/12/263/s1: Table S1: Composition of the reaction gas mixtures comprising single alkanes or natural gas alkanes in 75% inert gas; Table S2: Composition of the reaction gas mixtures comprising binary in 75% inert gas; Figure S1. XRD patterns obtained from $Rh1/Al_2O_3$, the support precursor ($\gamma-$AlOOH), and the pure support (mixture of γ-, θ- and δ-alumina phases); Figure S2. (a) CH_4 and (b) H_2 volumetric gas contents (water and inert gas excluded), (c) CO/COx ratio, and d) H_2/CO ratio in the steam reforming of methane over Rhx/Al_2O_3 at various Rh loadings (S/C = 4); Figure S3. (a) CH_4 and (b) H_2 volumetric gas contents (water and inert gas excluded), (c) CO/COx ratio, and (d) H_2/CO ratio in the steam reforming of methane over $Rh_{0.5}/Al_2O_3$ at various Rh loadings at various GHSVs (S/C = 4); Figure S4. H_2 volumetric gas contents (water and inert gas excluded) in the steam reforming of C_2–C_4 alkanes in mixture with methane over $Rh1/Al_2O_3$ at 350 °C and S/C of (a) 1, (b) 2.5 and (c) 4; Figure S5. H_2/CO ratios in the steam reforming of C_2–C_4 alkanes in mixture with methane over $Rh1/Al_2O_3$ at 350 °C and S/C of (a) 1, (b) 2.5 and (c) 4; Figure S6. Volumetric gas contents of permeate gas from membrane pre-separation and after subsequent steam reforming at 350 °C and a S/C ratio of 4 over $Rh1/Al_2O_3$ and commercial catalysts; Figure S7. H_2 volumetric gas contents (water and inert gas excluded) in the steam reforming of methane over $Rh1/Al_2O_3$ at various temperatures and S/C ratios of (a) 1,(b) 2.5 and (c) 4; Figure S8. H_2/CO ratios in the product gases in the steam reforming of methane over $Rh1/Al_2O_3$ at various temperatures and S/C ratios of (a) 1, (b) 2.5 and (c) 4; Figure S9. Volumetric CO- and CO_2-contents in the product gases (water and inert gas excluded) in the steam reforming of methane over $Rh1/Al_2O_3$ at various temperatures and S/C ratios of (a) 1, (b) 2.5 and (c) 4.

Author Contributions: Conceptualization, D.S. and S.W.; methodology, D.S., R.D. and S.W.; investigation, D.S., R.D., H.A. (Hanan Atia), H.A. (Hadis Amani), M.-M.P., G.G., S.K.; writing—original draft preparation, D.L.; writing—review and editing, D.S., D.L. and S.W.; supervision, S.W.

Funding: This research was partially funded by Sino-German (CSC-DAAD) Postdoc Scholarship Program (57251553) funded by CSC (China Scholarship Council), DAAD (Deutscher Akademischer Austausch Dienst).

Conflicts of Interest: The authors declare no conflict of interest.

References

1. McFarland, E. Unconventional Chemistry for Unconventional Natural Gas. *Science* **2012**, *338*, 340–342. [CrossRef]
2. Tang, P.; Zhu, Q.; Wu, Z.; Ma, D. Methane activation: The past and future. *Energy Environ. Sci.* **2014**, *7*, 2580–2591. [CrossRef]
3. Horn, R.; Schlögl, R. Methane Activation by Heterogeneous Catalysis. *Catal. Lett.* **2015**, *145*, 23–39. [CrossRef]
4. Olivos-Suarez, A.I.; Szécsényi, À.; Hensen, E.J.M.; Ruiz-Martinez, J.; Pidko, E.A.; Gascon, J. Strategies for the Direct Catalytic Valorization of Methane Using Heterogeneous Catalysis: Challenges and Opportunities. *ACS Catal.* **2016**, *6*, 2965–2981. [CrossRef]
5. Schwach, P.; Pan, X.; Bao, X. Direct Conversion of Methane to Value-Added Chemicals over Heterogeneous Catalysts: Challenges and Prospects. *Chem. Rev.* **2017**, *117*, 8497–8520. [CrossRef]
6. Kondratenko, E.V.; Peppel, T.; Seeburg, D.; Kondratenko, V.A.; Kalevaru, N.; Martin, A.; Wohlrab, S. Methane conversion into different hydrocarbons or oxygenates: Current status and future perspectives in catalyst development and reactor operation. *Catal. Sci. Technol.* **2017**, *7*, 366–381. [CrossRef]
7. Ross, J.R.H.; van Keulen, A.N.J.; Hegarty, M.E.S.; Seshan, K. The catalytic conversion of natural gas to useful products. *Catal. Today* **1996**, *30*, 193–199. [CrossRef]
8. Lunsford, J.H. Catalytic conversion of methane to more useful chemicals and fuels: A challenge for the 21st century. *Catal. Today* **2000**, *63*, 165–174. [CrossRef]
9. Aasberg-Petersen, K.; Dybkjær, I.; Ovesen, C.V.; Schjødt, N.C.; Sehested, J.; Thomsen, S.G. Natural gas to synthesis gas—Catalysts and catalytic processes. *J. Nat. Gas Sci. Eng.* **2011**, *3*, 423–459. [CrossRef]

10. Baliban, R.C.; Elia, J.A.; Weekman, V.; Floudas, C.A. Process synthesis of hybrid coal, biomass, and natural gas to liquids via Fischer–Tropsch synthesis, ZSM-5 catalytic conversion, methanol synthesis, methanol-to-gasoline, and methanol-to-olefins/distillate technologies. *Comput. Chem. Eng.* **2012**, *47*, 29–56. [CrossRef]
11. Wender, I. Reactions of synthesis gas. *Fuel Process. Technol.* **1996**, *48*, 189–297. [CrossRef]
12. Song, X.P.; Guo, Z.C. Technologies for direct production of flexible H_2/CO synthesis gas. *Energy Convers. Manag.* **2006**, *47*, 560–569. [CrossRef]
13. Rostrup-Nielsen, J.R. New aspects of syngas production and use. *Catal. Today* **2000**, *63*, 159–164. [CrossRef]
14. Joensen, F.; Rostrup-Nielsen, J.R. Conversion of hydrocarbons and alcohols for fuel cells. *J. Power Sources* **2002**, *105*, 195–201. [CrossRef]
15. Avcı, A.K.; Trimmb, D.L.; Aksoylu, A.E.; Önsan, Z.I. Hydrogen production by steam reforming of *n*-butane over supported Ni and Pt-Ni catalysts. *Appl. Catal. A* **2004**, *258*, 235–240. [CrossRef]
16. Hotz, N.; Stutz, M.J.; Loher, S.; Stark, W.J.; Poulikakos, D. Syngas production from butane using a flame-made $Rh/Ce_{0.5}Zr_{0.5}O_2$ catalyst. *Appl. Catal. B* **2007**, *73*, 336–344. [CrossRef]
17. Von Rickenbach, J.; Nabavi, M.; Zinovik, I.; Hotz, N.; Poulikakos, D. A detailed surface reaction model for syngas production from butane over Rhodium catalyst. *Int. J. Hydrogen Energy* **2011**, *36*, 12238–12248. [CrossRef]
18. Pasel, J.; Wohlrab, S.; Kreft, S.; Rotov, M.; Löhken, K.; Peters, R.; Stolten, D. Routes for deactivation of different autothermal reforming catalysts. *J. Power Sources* **2016**, *325*, 51–63. [CrossRef]
19. Auprêtre, F.; Descorme, C.; Duprez, D. Bio-ethanol catalytic steam reforming over supported metal catalysts. *Catal. Commun.* **2002**, *3*, 263–267. [CrossRef]
20. Schädel, B.T.; Duisberg, M.; Deutschmann, O. Steam reforming of methane, ethane, propane, butane, and natural gas over a rhodium-based catalyst. *Catal. Today* **2009**, *142*, 42–51. [CrossRef]
21. Karakaya, C.; Maier, L.; Deutschmann, O. Surface Reaction Kinetics of the Oxidation and Reforming of CH_4 over Rh/Al_2O_3 Catalysts. *Int. J. Chem. Kinet.* **2016**, *48*, 144–160. [CrossRef]
22. Angeli, S.D.; Monteleone, G.; Giaconia, A.; Lemonidou, A.A. State-of-the-art catalysts for CH_4 steam reforming at low temperature. *Int. J. Hydrogen Energy* **2014**, *39*, 1979–1997. [CrossRef]
23. Supat, K.; Chavadej, S.; Lobban, L.L.; Mallinson, R.G. Combined Steam Reforming and Partial Oxidation of Methane to Synthesis Gas under Electrical Discharge. *Ind. Eng. Chem. Res.* **2003**, *42*, 1654–1661. [CrossRef]
24. Bakker, W.J.W.; Kapteijn, F.; Poppe, J.; Moulijn, J.A. Permeation characteristics of a metal-supported silicalite-1 zeolite membrane. *J. Membr. Sci.* **1996**, *117*, 57–78. [CrossRef]
25. Krishna, R.; Vandenbroeke, L.J.P. The Maxwell-Stefan Description of Mass-Transport across Zeolite Membranes. *Chem. Eng. J. Biochem. Eng. J.* **1995**, *57*, 155–162. [CrossRef]
26. Vroon, Z.A.E.P.; Keizer, K.; Gilde, M.J.; Verweij, H.; Burggraaf, A.J. Transport properties of alkanes through ceramic thin zeolite MFI membranes. *J. Membr. Sci.* **1996**, *113*, 293–300. [CrossRef]
27. Keizer, K.; Burggraaf, A.J.; Vroon, Z.A.E.P.; Verweij, H. Two component permeation through thin zeolite MFI membranes. *J. Membr. Sci.* **1998**, *147*, 159–172. [CrossRef]
28. Van de Graaf, J.M.; Kapteijn, F.; Moulijn, J.A. Methodological and operational aspects of permeation measurements on silicalite-1 membranes. *J. Membr. Sci.* **1998**, *144*, 87–104. [CrossRef]
29. Gump, C.J.; Lin, X.; Falconer, J.L.; Noble, R.D. Experimental configuration and adsorption effects on the permeation of C_4 isomers through ZSM-5 zeolite membranes. *J. Membr. Sci.* **2000**, *173*, 35–52. [CrossRef]
30. Arruebo, M.; Coronas, J.; Menendez, M.; Santamaria, J. Separation of hydrocarbons from natural gas using silicalite membranes. *Sep. Purif. Technol.* **2001**, *25*, 275–286. [CrossRef]
31. Wohlrab, S.; Meyer, T.; Stöhr, M.; Hecker, C.; Lubenau, U.; Oßmann, A. On the performance of customized MFI membranes for the separation of *n*-butane from methane. *J. Membr. Sci.* **2011**, *369*, 96–104. [CrossRef]
32. Dragomirova, R.; Stohr, M.; Hecker, C.; Lubenau, U.; Paschek, D.; Wohlrab, S. Desorption-controlled separation of natural gas alkanes by zeolite membranes. *RSC Adv.* **2014**, *4*, 59831–59834. [CrossRef]
33. Neubauer, K.; Dragomirova, R.; Stöhr, M.; Mothes, R.; Lubenau, U.; Paschek, D.; Wohlrab, S. Combination of membrane separation and gas condensation for advanced natural gas conditioning. *J. Membr. Sci.* **2014**, *453*, 100–107. [CrossRef]
34. Dragomirova, R.; Jorabchi, M.N.; Paschek, D.; Wohlrab, S. Operational Criteria for the Separation of Alkanes by Zeolite Membranes. *Chem. Ing. Tech.* **2017**, *89*, 926–934. [CrossRef]

35. Angeli, S.D.; Pilitsis, F.G.; Lemonidou, A.A. Methane steam reforming at low temperature: Effect of light alkanes' presence on coke formation. *Catal. Today* **2015**, *242*, 119–128. [CrossRef]
36. Guo, X.; Fang, G.; Li, G.; Ma, H.; Fan, H.; Yu, L.; Ma, C.; Wu, X.; Deng, D.; Wei, M.; et al. Direct, Nonoxidative Conversion of Methane to Ethylene, Aromatics, and Hydrogen. *Science* **2014**, *344*, 616–619. [CrossRef] [PubMed]
37. Huang, W.; Zhang, S.; Tang, Y.; Li, Y.; Nguyen, L.; Li, Y.; Shan, J.; Xiao, D.; Gagne, R.; Frenkel, A.I.; et al. Low-Temperature Transformation of Methane to Methanol on Pd_1O_4 Single Sites Anchored on the Internal Surface of Microporous Silicate. *Angew. Chem.* **2016**, *128*, 13639–13643. [CrossRef]
38. Vanelderen, P.; Vancauwenbergh, J.; Tsai, M.-L.; Hadt, R.G.; Solomon, E.I.; Schoonheydt, R.A.; Sels, B.F. Spectroscopy and Redox Chemistry of Copper in Mordenite. *Chem. Phys. Chem.* **2014**, *15*, 91–99. [CrossRef]
39. Grundner, S.; Markovits, M.A.C.; Li, G.; Tromp, M.; Pidko, E.A.; Hensen, E.J.M.; Jentys, A.; Sanchez-Sanchez, M.; Lercher, J.A. Single-site trinuclear copper oxygen clusters in mordenite for selective conversion of methane to methanol. *Nat. Commun.* **2015**, *6*, 7546. [CrossRef]
40. Grundner, S.; Luo, W.; Sanchez-Sanchez, M.; Lercher, J.A. Synthesis of single-site copper catalysts for methane partial oxidation. *Chem. Commun.* **2016**, *52*, 2553–2556. [CrossRef]
41. Kulkarni, A.R.; Zhao, Z.-J.; Siahrostami, S.; Nørskov, J.K.; Studt, F. Monocopper Active Site for Partial Methane Oxidation in Cu-Exchanged 8MR Zeolites. *ACS Catal.* **2016**, *6*, 6531–6536. [CrossRef]
42. Wallis, P.; Schonborn, E.; Kalevaru, V.N.; Martin, A.; Wohlrab, S. Enhanced formaldehyde selectivity in catalytic methane oxidation by vanadia on Ti-doped SBA-15. *RSC Adv.* **2015**, *5*, 69509–69513. [CrossRef]
43. Wallis, P.; Wohlrab, S.; Kalevaru, V.N.; Frank, M.; Martin, A. Impact of support pore structure and morphology on catalyst performance of VO_x/SBA-15 for selective methane oxidation. *Catal. Today* **2016**, *278*, 120–126. [CrossRef]
44. Dang, T.T.H.; Seeburg, D.; Radnik, J.; Kreyenschulte, C.; Atia, H.; Vu, T.T.H.; Wohlrab, S. Influence of V-sources on the catalytic performance of VMCM-41 in the selective oxidation of methane to formaldehyde. *Catal. Commun.* **2018**, *103*, 56–59. [CrossRef]
45. Duarte, R.B.; Krumeich, F.; van Bokhoven, J.A. Structure, Activity, and Stability of Atomically Dispersed Rh in Methane Steam Reforming. *ACS Catal.* **2014**, *4*, 1279–1286. [CrossRef]
46. Lian, J.; Ma, J.; Duan, X.; Kim, T.; Li, H.; Zheng, W. One-step ionothermal synthesis of g-Al_2O_3 mesoporous nanoflakes at low temperature. *Chem. Commun.* **2010**, *46*, 2650–2652. [CrossRef]
47. Fargeot, D.; Mercurio, D.; Dauger, A. Structural characterization of alumina metastable phases in plasma sprayed deposits. *Mater. Chem. Phys.* **1990**, *24*, 299–314. [CrossRef]
48. Husson, E.; Repelin, Y. Structural studies of transition aluminas. Theta alumina. *Eur. J. Solid State Inorg. Chem.* **1996**, *33*, 1223–1231.
49. Weng, W.Z.; Pei, X.Q.; Li, H.M.; Luo, C.R.; Liu, Y.; Lin, H.Q.; Huang, C.J.; Wan, H.L. Effects of calcination temperatures on the catalytic performance of Rh/Al_2O_3 for methane partial oxidation to synthesis gas. *Catal. Today* **2006**, *117*, 53–61. [CrossRef]
50. Yao, H.C.; Japar, S.; Shelef, M. Surface interactions in the system $RhAl_2O_3$. *J. Catal.* **1977**, *50*, 407–418. [CrossRef]
51. Guan, H.L.; Lin, J.; Qiao, B.T.; Miao, S.; Wang, A.Q.; Wang, X.D.; Zhang, T. Enhanced performance of Rh_1/TiO_2 catalyst without methanation in water-gas shift reaction. *AIChE J.* **2017**, *63*, 2081–2088. [CrossRef]
52. Graf, P.O.; Mojet, B.L.; van Ommen, J.G.; Lefferts, L. Comparative study of steam reforming of methane, ethane and ethylene on Pt, Rh and Pd supported on yttrium-stabilized zirconia. *Appl. Catal. A* **2007**, *332*, 310–317. [CrossRef]
53. Igarashi, A.; Ohtaka, T.; Motoki, S. Low-temperature steam reforming of *n*-butane over Rh and Ru catalysts supported on ZrO_2. *Catal. Lett.* **1992**, *13*, 189–194. [CrossRef]
54. Alcheikhhamdon, Y.; Hoorfar, M. Natural gas quality enhancement: A review of the conventional treatment processes, and the industrial challenges facing emerging technologies. *J. Nat. Gas Sci. Eng.* **2016**, *34*, 689–701. [CrossRef]
55. Dragomirova, R.; Wohlrab, S. Zeolite Membranes in Catalysis—From Separate Units to Particle Coatings. *Catalysts* **2015**, *5*, 2161–2222. [CrossRef]

56. Krishna, R.; Paschek, D. Separation of hydrocarbon mixtures using zeolite membranes: A modelling approach combining molecular simulations with the Maxwell–Stefan theory. *Sep. Purif. Technol.* **2000**, *21*, 111–136. [CrossRef]
57. Hansen, T.W.; DeLaRiva, A.T.; Challa, S.R.; Datye, A.K. Sintering of Catalytic Nanoparticles: Particle Migration or Ostwald Ripening? *Acc. Chem. Res.* **2013**, *46*, 1720–1730. [CrossRef] [PubMed]